Available online at www.sciencedirect.com
ScienceDirect
Thin Solid Films 516 (2008) 6668–6672
www.elsevier.com/locate/tsf

Magnetized microdischarge plasma generation at low pressure

Tsuyohito Ito [a,*], Kazunobu Kobayashi [b], Satoshi Hamaguchi [b], Mark A. Cappelli [c]

[a] Frontier Research Base for Global Young Researchers, Frontier Research Center, Graduate School of Engineering, Osaka University, 2-1 Yamadaoka, Suita, Osaka 565-0871, Japan
[b] Center for Atomic and Molecular Technologies, Graduate School of Engineering, Osaka University, 2-1 Yamadaoka, Suita, Osaka 565-0871, Japan
[c] Mechanical Engineering Department, Stanford University, Stanford, CA 94305-3032, USA

Available online 19 November 2007

Abstract

A magnetized microdischarge plasma is generated at low pressure with planar electrodes and a non-uniform magnetic field configuration causing closed $\mathbf{E}\times\mathbf{B}$ electron drift. Stable generation with a 1 mm electrode gap has been achieved in 0.5–55 Torr of argon. The breakdown voltage curve is found to have two local minima, the lower of which is believed to be caused by strong electron magnetization, as supported by simple Monte Carlo simulations. The current–voltage curves show strong variations between operation at 10 Torr and lower pressures. The plasma confinement, as inferred from the luminous emission of the annular-shape discharge, appears to be stronger at low pressures. Optical emission is used to infer electron excitation temperatures, which are estimated to be about 1 eV.

Keywords: Microdischarge; Magnetized plasma; Low pressure

1. Introduction

There is a growing interest in the development of micro-plasmas, microdischarges, or micro-ion sources for a range of applications, such as local etch processing [1], chemical analysis [2], materials synthesis [3,4], surface treatment/modification [5], and sterilization [6]. A common feature of microdischarges is that they can be ignited and sustained at relatively high pressure, removing the need, in some cases, for vacuum chambers. However, a trade-off of this is the operation in a highly collisional environment, which precludes applications that may require high ion energy. The generation and operation of a microdischarge at low pressures and low powers may open fields of applications that benefit from focused, high current density, and highly energetic ions, such as in spatially constrained surface treatment or modification, sputtering, low energy ion implantation, and micropropulsion. By the application of a magnetic field, we have demonstrated microdischarge generation at low pressure [7] and its application to the development of a micropropulsion device [8].

In this paper, we present initial measurements and simulations of a magnetized microdischarge plasma with planar electrodes and a non-uniform magnetic field configuration promoting closed $\mathbf{E}\times\mathbf{B}$ electron drift.

2. Experimental details

2.1. Magnetized microdischarge plasma generation

Fig. 1 depicts the electrode and magnetic field configuration employed for breakdown voltage measurements and for visual observations of the discharge. The cathode is fabricated from aluminum and the anode is a thin film of indium tin oxide (ITO) on a transparent plastic sheet. Use of the transparent ITO anode allows us to observe the annular discharge along a direction perpendicular to the electrodes. The magnetic field is simulated using a two-dimensional axisymmetric finite element solver [9]. The magnetic circuit incorporates a ring-shaped SmCo permanent magnet together with a high purity iron core to form the magnetic poles. The outer diameter of the magnet is 14 mm, the inner diameter is 4 mm, and the thickness is 3 mm. The outer diameter of the iron core is 3 mm. With this configuration, the magnetic field strength near the cathode approaches ~1 Tesla, resulting in a Larmor radius of 10 μm for an electron energy of 10 eV. The

* Corresponding author. Tel.: +81 6 6879 7817; fax: +81 6 6879 7916.
E-mail address: tsuyohito@wakate.frc.eng.osaka-u.ac.jp (T. Ito).

0040-6090/$ - see front matter © 2007 Elsevier B.V. All rights reserved.
doi:10.1016/j.tsf.2007.11.040

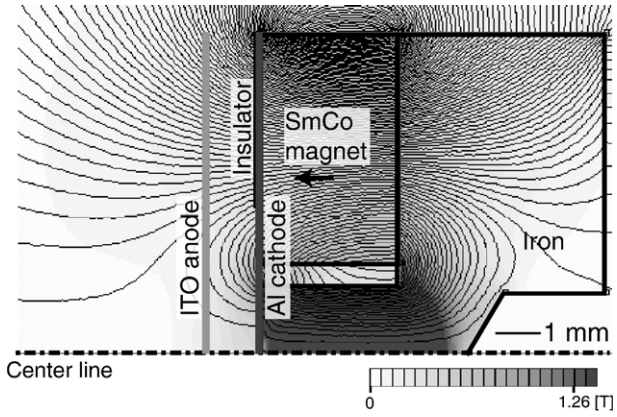

Fig. 1. Schematic of the discharge cross section.

discharge gap can be varied, but is fixed for the studies reported here at 1 mm. The microdischarge was generated in an argon (Ar).

Monte Carlo (MC) simulations of electron trajectories were performed to facilitate a better understanding of the breakdown process. In these simulations, electrons are introduced with zero energy at random locations on the cathode and their trajectories in response to the imposed uniform axial electric field and non-uniform magnetic field are computed using a leap-frog method. The simulation is three-dimensional (3D) in the cylindrical volume between electrodes with the maximum radial domain boundary at 4 mm. The gap voltage is 250 V. The time step used to advance the electrons is 10^{-14} s. The emitted electrons lead to avalanche ionization, and the number and location of these ionization events are recorded within radial cells spaced by about 0.1 mm over the electrode radius of about 3 mm. One hundred electrons are initially introduced from the cathode into each radial cell. The elastic and non-elastic electron-neutral cross sections used in the simulation are those reported by Phelps [10].

2.2. Current–voltage characteristics and optical emission studies

The current–voltage (I–V) characteristics and optical emission measurements are carried out with a discharge configuration that is slightly different from that shown in Fig. 1. Here, the material for both electrodes is copper (Cu). The outer diameter of the SmCo magnet is 17 mm, the inner diameter is 5 mm, the thickness is 5 mm, and the outer diameter of the iron core is 4 mm. The discharge current is measured by recording the voltage across a ballast (10 kΩ) resistor located between the power supply and the powered electrode (cathode).

Optical emission spectroscopy is performed by analyzing the spectrum of light emitted from the luminous annular discharge as viewed along a direction parallel to the electrode's surface. The emission is focused onto an optical fiber and coupled to a CCD spectrometer (Ocean Optics model HR4000) using a convex lens with the focal length of 5 cm. The object and image distances are approximately 9 cm and 11 cm respectively. Spectral line interferences precluded the use of Ar lines to estimate electronic excitation temperatures. However spectral line emission from Cu, which originates through electron impact excitation of Cu sputtered from the electrodes, is detected, well-resolved, and prevalent at low discharge pressures. Four Cu emission lines, listed in Table 1 [11] with three upper electronic states are used for estimating the electronic excitation temperature. The close proximity in wavelength of these transitions allows us to determine relative intensity without having to calibrate the spectral sensitivity of the spectrometer. The emission originating from the highest state is weak and not detected in most operating conditions (shown in Fig. 6 below). As a result, in most cases, the temperature reported is based on the use of three lines originating from two upper energy states.

Table 1
Copper lines employed for estimating excitation temperatures

Wavelength [nm]	Energy levels [eV]	A coefficient [10^6 s^{-1}]	Degeneracy
510.5	3.82	2	4
515.3	6.19	60	4
521.8	6.19	75	6
529.3	7.74	10.9	8

3. Results and discussion

3.1. Magnetized microdischarge plasma generation

Photographs of the generated plasma as viewed through the ITO anode are shown in Fig. 2. At low pressure (e.g. Fig. 2a, 1 Torr) we see the presence of a clear annular-shaped microdischarge with

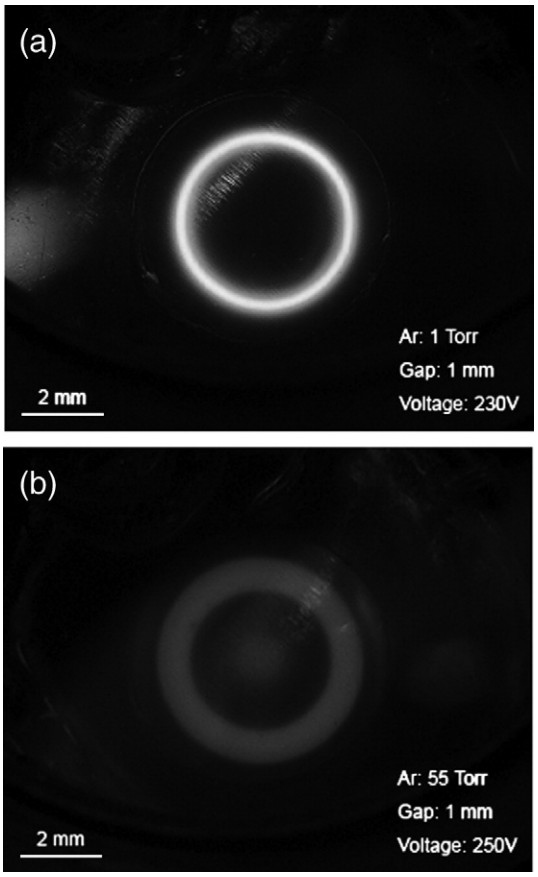

Fig. 2. Photographs of the magnetized microdischarge plasmas. These pictures were taken with the same camera setting through the ITO anode.

strong emission from regions where the magnetic field is strongest. In contrast, when operating at high pressure (e.g., Fig. 2b — 55 Torr), we see, in addition to a more diffuse annular glow, a luminous glow centered about the axis where the magnetic field is almost parallel to the electric field. While the sharpness of the annulus appears to be stronger at lower pressure (suggesting better plasma confinement), no discernable differences are seen at pressures lower than ~5 Torr. The transition, from a diffuse annular emission to a clear annular emission, is indicative of the strong influence of the magnetic field on the discharge with diminishing pressure.

3.2. Breakdown voltages

The breakdown voltage curve is shown in Fig. 3. In the absence of a magnetic field, the minimum in the breakdown voltage is expected to be close to 15 mm Torr. The results of the MC simulations without a magnetic field are also shown in Fig. 3 for comparison. This MC simulation for predicting breakdown is based on the usual Townsend breakdown criteria (balance between ionization and secondary electron emission), and is carried out in one-dimension (1D). A secondary electron emission coefficient γ of 0.03 is used to obtain the best agreement with the experiments in the high pressure region, where the effect of the magnetic field is expected to be small. The minimum breakdown voltage depends on the choice of γ, and we find that with a value of $\gamma = 0.01$–0.1, the simulations result in a range of minima in the breakdown voltage (e.g., 230 V at 20 mm Torr for and $\gamma = 0.01$, and 130 V at 10 mm Torr for $\gamma = 0.1$). We see that the experimental data of breakdown voltage in the presence of a magnetic field also shows a minimum near 15 mm Torr. We attribute this minimum, which is consistent with that expected in the absence of a magnetic field, to the magnetic field non-uniformity and the presence of a region between the electrodes where the magnetic field is perpendicular to the electrodes (i.e., parallel to the electric field). At these higher pressures, the breakdown behavior is also concomitant with the presence of the weak emission close to the axis, as seen in Fig. 2b. In the region of low magnetic field under high pressure conditions, the electrons will experience many collisions within a field gyration (the mean free path is about 20 μm at 15 Torr using the cross section of 10^{-19} m^2), and so that the magnetic field is less effective at confining the electron motion. An examination of the breakdown curve shows that a more interesting feature exists at lower pressure. We see the presence of a second minimum near a pressure of 1 Torr, where the mean free path is about 300 μm. We believe that the minimum is a clear indicator that electrons are strongly magnetized, since the decrease in breakdown voltage is caused by the longer electron trajectory, resulting in a higher collision probability and more electron avalanche ionization cascades.

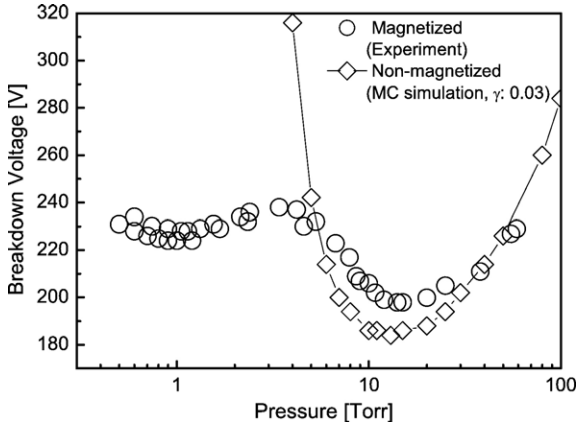

Fig. 3. Breakdown voltage as a function of pressure: Ar environment, 1 mm gap.

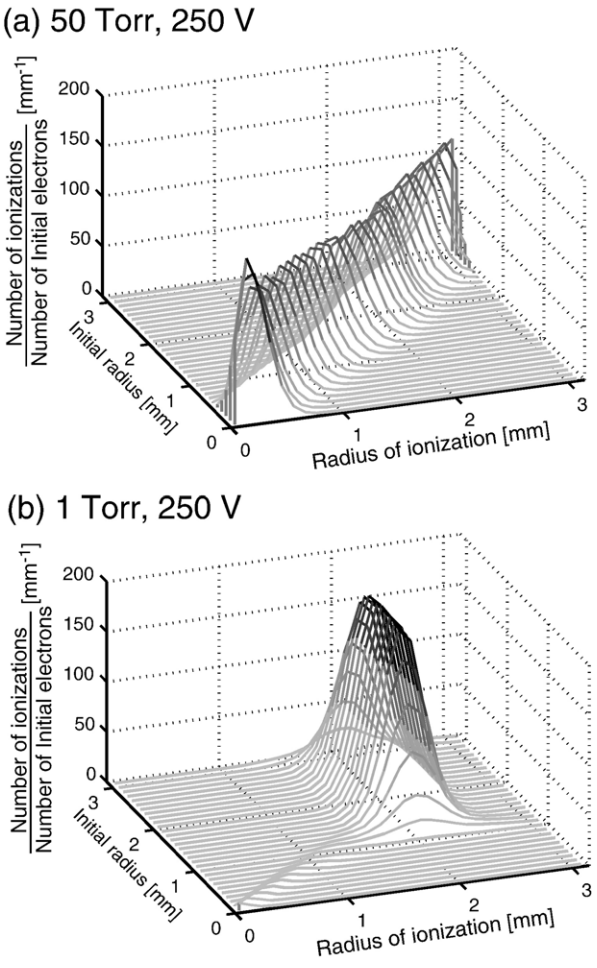

Fig. 4. Monte Carlo simulation results of radial distributions of ionization events as the function of radius positions of initial electrons; a: 50 Torr, b: 1 Torr. The gap voltage is 250 V.

Results of the MC simulations of electron trajectories under magnetized conditions are shown in Fig. 4. Here we depict the number and location of ionization events, for electrons released from varying radial positions on the cathode. For the high pressure, 50 Torr condition (Fig. 4a), electrons seem to travel to the anode along a direction almost parallel to the electric field, resulting in ionization at radial locations close to where they were emitted from the cathode (i.e., $R_{\text{initial}} \approx R_{\text{ionization}}$). We also see that the amount of ionization attributable to a single electron is almost independent of the initial radius, although the magnetic field strength and direction vary strongly with radius. In contrast, the predictions are considerably different at lower

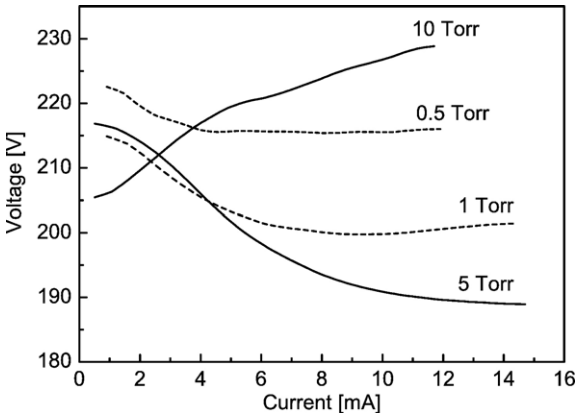

Fig. 5. Current–voltage characteristics.

pressure, i.e., at 1 Torr (see Fig. 4b). It is apparent that electron emission near the axis, where the magnetic field is parallel to the electric field, does not lead to a large number of ionization events, due to the poor electron confinement and therefore very few collision opportunities. However, initial electron release at a radius of 1–3 mm creates significant ionization near the 2 mm radius in regions of strong magnetic field perpendicular to the electric field, as seen in Fig. 1.

3.3. Current–voltage characteristics

Fig. 5 shows the current–voltage (I–V) characteristics recorded with the Cu electrodes and the larger magnet. We see a transition from a negative to positive resistance between the 5 Torr and 10 Torr conditions. Although a quantitative measurement has not yet been performed, the current density at lower pressure may be higher (for the same total current) than that at 10 Torr, since the plasma is more concentrated at lower pressure. No discernable differences in discharge shape are seen as pressures are reduced below 5 Torr. We do see that lower voltage operation results in a higher current density for low pressures relative to that at 10 Torr, in contrast with the usual Jn^{-2} (here, J is the current density and n is the particle density) scaling in the absence of a magnetic field. This departure is expected at lower pressures, where the electrons are highly magnetized.

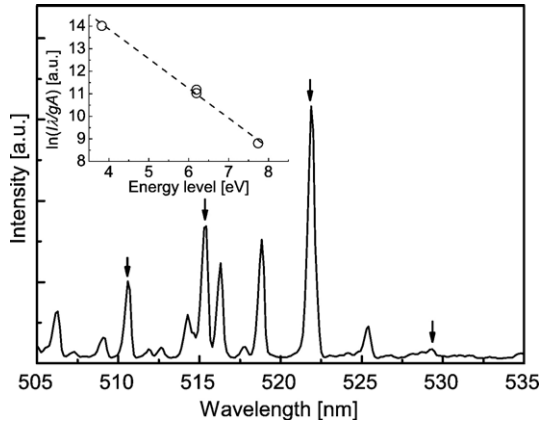

Fig. 6. Emission spectrum at 505–535 nm and Boltzmann plot for estimating the excitation temperature of Cu. The conditions are 1 Torr, 196 V, and 10.0 mA.

Table 2
Estimated electronic excitation temperatures of Cu

Pressure [Torr]	Voltage [V]	Current [mA]	Excitation temperature [eV]
10	230	10.0	0.95
1	204	3.0	1.28
1	197	5.0	0.92
1	194	7.0	0.85
1	196	10.0	0.81 (0.76)
0.5	213	5.0	1.17
0.5	214	7.0	0.92
0.5	216	9.9	0.86

The value in the parenthesis indicates a temperature from the three energy states.

Slow drifts in the I–V curves are seen in some conditions during the experiments. We attribute these drifts to changes in the electrode surface condition. The high plasma density concentrated in an annulus, especially at low pressure, results in sputtering of the cathode material. We eliminated the effect of thermal drifts arising from a gradual temperature rise in the magnetic circuit by sweeping the applied voltage at relatively high rates (50 V/s). In all cases, I–V curves were obtained with relatively new electrodes and there was no detectable hysteresis associated with the direction of the voltage sweep.

3.4. Electronic excitation temperature

In an attempt to better understand the I–V behavior at low pressure, we have carried out measurements of the electron excitation temperature. Fig. 6 shows a representative optical emission spectrum detected over the 505 nm–535 nm range, with arrows identifying the four Cu transitions studied. Superimposed as an inset to the figure is a typical Boltzmann plot used for estimating the electronic excitation temperatures of Cu. Table 2 lists these estimated excitation temperatures, for pressures ranging range 0.5–10 Torr, and voltages of 216 V–230 V respectively. The excitation temperatures are found to be approximately 1 eV for most cases, with a tendency to decrease slightly with increased current density. No obvious sudden changes in excitation temperature, which might reflect changes in the electron energy distribution, are seen with increasing pressure to 10 Torr. Understanding this transition from positive to negative resistance will require further study, and is the subject of future research.

4. Conclusions

A magnetized annular microdischarge plasma has been generated at low pressure using planar electrodes and a non-uniform magnetic field configuration which causes closed $\mathbf{E}\times\mathbf{B}$ electron drift. The breakdown voltage characteristic is found to have two local minima. The lower minimum, near a pressure of 1 Torr, is believed to be indicative of strong electron magnetization, a result also supported by simple Monte Carlo simulations. Significant differences are seen in the current–voltage curves as pressure is reduced to below 10 Torr. Although quantitative measurements of discharge current density have not yet been made, the scaling of the I–V characteristics at low pressure departs from that

in the absence of a magnetic field, as expected due to the strong magnetization. The electronic excitation temperature has been estimated to be approximately 1 eV, and seems to be insensitive to pressure below 10 Torr. Local sputtering of the cathode has been observed as a result of the strong confinement of the plasma, particularly at low pressure. This small discharge, which can be operated stably in argon at pressures as low as 0.5 Torr, may be useful as small energetic ion sources for sputtering or localized surface modification. The compact nature of this source allows for clustering of multi-ion sources. Future research includes measurements of the local ion current density, cathode sputter rate, as well as characterization of the plasma density and electron temperature, especially at lower pressure where there seems to be a transition from positive to negative resistance.

Acknowledgments

The authors would like to thank W. S. Crawford and K. Karahashi for technical support. This research has been funded in part by the National Science Foundation. Part of this research has been carried out at the Frontier Research Base for Global Young Researchers, Osaka University, through the program Promotion of Environmental Improvement to Enhance Young Researchers' Independence, the special coordination funds for promoting science and technology, Japan ministry of education, culture, sports, science and technology.

References

[1] R.M. Sankaran, K.P. Giapis, Appl. Phys. Lett. 79 (2001) 593.
[2] C. Brede, S.P. -Bjergaard, E. Lundanes, T. Greibrokk, Anal. Chem. 70 (1998) 513.
[3] T. Ito, T. Izaki, K. Terashima, Thin Solid Films 386 (2001) 300.
[4] Y. Shimizu, T. Sasaki, A.C. Bose, K. Terashima, N. Koshizaki, Surf. Coat. Technol. 200 (2006) 4251.
[5] H. Yoshiki, A. Oki, H. Ogawa, Y. Horiike, J. Vac. Sci. Technol., A, Vac. Surf. Films 20 (2002) 24.
[6] R. Rahul, O. Stan, A. Rahman, E. Littlefield, K. Hoshimiya, A.P. Yalin, A. Sharma, A. Pruden, C.A. Moore, Z. Yu, G.J. Collins, J. Phys., D, Appl. Phys. 38 (2005) 1750.
[7] T. Ito, M.A. Cappelli, Appl. Phys. Lett. 89 (2006) 061501.
[8] T. Ito, N. Gascon, W.S. Crawford, M.A. Cappelli, J. Propuls. Power 23 (2007) 1068.
[9] D.C. Meeker, Finite Element Method Magnetics, Version 3.4.1, http://femm.foster-miller.net.
[10] A.V. Phelps, Private communication. http://jilawww.cololado.edu/~avp/.
[11] NIST atomic spectra database. http://physics.nist.gov/PhysRefData/ASD/index.html.